energies

MDPI

Article

High Load Compression Ignition of Wet Ethanol Using a Triple Injection Strategy

Brian Gainey *, Ziming Yan, John Gandolfo and Benjamin Lawler

Department of Automotive Engineering, Clemson University, 4 Research Drive, Greenville, SC 29607, USA; zimingy@clemson.edu (Z.Y.); gandolf@clemson.edu (J.G.); bjlawle@clemson.edu (B.L.)
* Correspondence: bgaine2@g.clemson.edu

Abstract: Wet ethanol is a biofuel that can be rapidly integrated into the existing transportation sector infrastructure and have an immediate impact on decarbonization. Compared to conventional hydrocarbon fuels, wet ethanol has unique fuel properties (e.g., short carbon chain, oxygenated, high heat of vaporization, no cool-flame reactivity), which can actually improve the efficiency and engine-out emissions of internal combustion engines while decarbonizing. In this work, wet ethanol 80 (80% ethanol, 20% water by mass) was experimentally studied at high loads under boosted conditions in compression ignition to study the tradeoffs in efficiency and emissions based on boosting and injection strategies. Specifically, this work explores the potential of adding a third, mixing-controlled injection at high loads. The results indicate that adding a third, mixing-controlled injection results in combustion stabilization at high loads, where the peak pressure limit of the engine is a constraint that requires combustion phasing to retard. However, since the heat of vaporization of wet ethanol 80 is ~6% of its lower heating value, evaporation of fuel injected near top dead center imposes a thermodynamic efficiency penalty by absorbing heat from the working fluid at a time in the cycle when adding heat produces net work out. Additionally, the mixing-controlled injection increases NOx emissions. Therefore, the amount of fuel injected in the mixing-controlled injection should be limited to only what is necessary to stabilize combustion. Ultimately, by using wet ethanol 80 in a triple injection strategy, a load of 22 bar IMEPn is achieved with a net fuel conversion efficiency of 42.2%, an engine-out indicated specific emissions of NOx of 1.3 g/kWh, and no measurable particulate matter, while maintaining a peak cylinder pressure below 150 bar.

Keywords: ethanol; wet ethanol; compression ignition; advanced compression ignition; biofuel

Citation: Gainey, B.; Yan, Z.; Gandolfo, J.; Lawler, B. High Load Compression Ignition of Wet Ethanol Using a Triple Injection Strategy. *Energies* **2022**, *15*, 3507. https://doi.org/10.3390/en15103507

Academic Editor: Dimitrios C. Rakopoulos

Received: 19 April 2022
Accepted: 7 May 2022
Published: 11 May 2022

1. Introduction

The production and combustion of a biofuel is considered part of the fast-carbon cycle, i.e., the carbon dioxide emissions produced from burning a biofuel were originally absorbed by the plants that produced the biofuel. In this way, a biofuel can be carbon-neutral, provided the production can be done responsibly. Although biofuels are not currently carbon-neutral, they currently have a significantly lower carbon intensity compared to fossil fuels and their carbon intensity can be lowered further in the near future as scale increases and technology matures [1]. As such, biofuels show promise as part of a renewable fuel economy to replace fossil fuels in the transportation sector [2], resulting in a sustainable and affordable future transportation solution for the developing and developed parts of the world.

Ethanol is a biofuel that warrants serious consideration as a leading renewable fuel. In order for a renewable fuel to be rapidly integrated into the existing transportation sector, it needs a mature production infrastructure and must function as a drop-in replacement for conventional fuels so that it can be used in existing vehicles with minor hardware modifications, at most. In a landscape of potential renewable fuels that includes green natural gas, hydrogen, ammonia, and synthetic hydrocarbons, alcohols like ethanol stand

out for a number of reasons. Ethanol is a liquid, is relatively non-toxic, and is of only moderate corrosiveness. Currently, ethanol is produced in large quantities from corn in the US and sugarcane in Brazil. Valid concerns over scaling these production infrastructures can be addressed in a number of ways: increasing crop utilization by using cellulose [3], decreasing fertilizer requirements by using crops that fix their own nitrogen [4], using underutilized resources like municipal waste [5], and algal farming [6]. The fermentation process also produces a stream of pure carbon dioxide, a resource quickly increasing in value as it is required to produce many e-fuels like methanol or synthetic hydrocarbons.

In the US, ethanol is typically blended into gasoline at 10% volume to both increase the biofuel content of the fuel and serve as an octane booster [7]. Ethanol is a very effective octane booster, specifically for boosted spark ignition engines [8]. Increasing the fraction of ethanol in gasoline would be a synergetic improvement to spark ignition engines by increasing the biofuel content of gasoline while also improving efficiency by enabling more spark advance and a higher compression ratio operation [9]. In order to blend ethanol in gasoline, water must be removed from the product of fermentation, which consists of ~13% ethanol in water. This water removal process is highly nonlinear in energy consumption and impacts the lifecycle efficiency of ethanol as an alternative fuel. If ethanol were to be used on its own as a single fuel instead of being blended with hydrocarbons that are not miscible with water, the water removal process could be truncated and the lifecycle efficiency could improve [10].

Ethanol forms an azeotrope with water at a concentration of 92.3% mass in water. Water removal beyond this azeotropic limit requires a mechanism transition from distillation to dehydration, which incurs a significant increase in complexity and energy consumption. In Brazil, azeotropic ethanol, also known as hydrous ethanol, is used in spark ignition engines to save some of the energy required to remove the water and improve the lifecycle efficiency of ethanol production [11]. If the water removal process were truncated earlier, wet ethanol, a pre-azeotropic blend of ethanol and water, can be directly used, which would save even more of the energy required to produce ethanol, thereby further improving the lifecycle carbon intensity of ethanol.

First-generation kinetically-controlled combustion strategies like homogeneous charge compression ignition (HCCI) demonstrated high-efficiency operation with near-zero NOx and particulate matter (PM) emissions [12]. Wet ethanol can be effectively employed in HCCI [13–15]. The heat release process in HCCI is dictated by natural thermal stratification formed from heat transfer during the compression stroke whereby the hottest regions in the cylinder achieve autoignition first, release their heat and further compress and heat the remaining colder regions in the cylinder, resulting in their autoignition. This process is called sequential autoignition and is a positive feedback process whose strength is a function of the thermal stratification level and the specific fuel-based energy density in the cylinder (i.e., equivalence ratio). As such, high-load operation of HCCI is limited by energy release rates that require excessive boosting and/or EGR to suppress. Researchers have used fuels with cool-flame reactivity to control the heat release process of kinetics-driven combustion via fuel stratification [16]. While effective, this approach requires fuels with high levels of cool-flame reactivity, and also requires sophisticated control strategies, since the cool-flame reactivity level of a fuel is highly sensitive to operating conditions such as temperature and boost level [17]. This difficulty has resulted in research focusing heavily on designer fuels [18] or relying on mixing-controlled combustion for compression ignition [19,20].

In advanced compression ignition (ACI) engines, wet ethanol has demonstrated the ability to enable kinetically-controlled combustion strategies with high controllability, high efficiency, and low criteria pollutants [21]. Wet ethanol has a high cooling potential due to its high heat of vaporization and low stoichiometric air-fuel ratio compared to traditional hydrocarbons [22]. Additionally, ethanol is a single-stage ignition fuel under all engine relevant operating conditions, including high-boost operation [23,24]. This makes wet ethanol and other wet, low carbon number alcohol fuels uniquely suited to enable highly

controllable kinetically-controlled combustion [22]. The unique fuel properties of wet ethanol allow it to enable control of kinetics-driven combustion that is not highly sensitive to operating conditions. When wet ethanol is injected during the compression stroke, the areas targeted by the spray are cooled by evaporation, resulting in an increase in thermal stratification. This slows the positive feedback process of sequential autoignition, lowering energy release rates to levels that are safe for engine health.

Previous work by the authors outline the effectiveness of wet ethanol in kinetically-controlled combustion using a split injection strategy, naming the strategy thermally stratified compression ignition (TSCI) [21]. The majority of the fuel is injected during the intake stroke to premix with the incoming air. A second injection delivers the remaining fuel during the middle of the compression stroke. The injection timing of both injections as well as the split fraction between the two injections have proven to be effective control knobs over the start and rate of combustion [25,26]. Previous work also showed that this strategy works best when coupled with an injector that can aim the compression stroke injection towards regions in the combustion chamber that have the highest local relative heat transfer rates, e.g., a wide spray angle aiming towards the squish region [27]. This allows the evaporative cooling to work with the natural thermal stratification, rather than against it, minimizing the required stratification and thereby minimizing NOx formation.

A solution to the control problem of kinetically-controlled combustion with gasoline is to employ a triple injection strategy, where the first injection premixes the fuel and air, the second injection partially premixes the fuel and air, and the third injection results in a mixing-controlled combustion phase of the heat release process, i.e., a diffusion flame normally associated with conventional diesel combustion or mixing-controlled compression ignition (MCCI) [28]. Some strategies eliminate the premixed injection altogether and focus on partially premixed and diffusion injections. In some sense, all advanced compression ignition strategies can be thought of as some combination of one or more of these three types of injections with the caveat that some strategies use multiple injections in the same category [29]. So, while wet ethanol does not require the "third" mixing-controlled injection, adding a mixing-controlled phase at very high loads is an available tool that has not been explored.

A significant amount of previous work involving ethanol considers either blending neat ethanol with diesel [30] or using neat ethanol with diesel in a dual-fuel application [31,32]. This work focuses on experimentally demonstrating high load operation of compression ignition with wet ethanol 80 (80% ethanol, 20% water, by mass) in a direct manner. Previous work demonstrated ACI of wet ethanol 80 up to a load of 8 bar net indicated mean effective pressure (IMEPn) [21]. Therefore, the goal of this study is to explore strategies to extend the load range further such that the full load range of spark ignition or diesel combustion can be covered with wet ethanol compression ignition. Two loads were studied in detail: 10 bar and 16 bar IMEPn. At 10 bar IMEPn, experiments were designed to answer questions related to emissions and efficiency tradeoffs of boost level on purely kinetically-controlled combustion with wet ethanol. At 16 bar IMEPn, the peak pressure limit of the engine was approached, and the addition of a third, mixing-controlled injection was studied. In this study, experiments and 0-D thermodynamic engine modeling were used together to gain an understanding of the thermodynamic effects of this mixing-controlled injection on the cycle. Finally, a load sweep is performed, demonstrating operating loads of up to 22 bar IMEPn with wet ethanol 80 in compression ignition, which constitutes the full operation range of modern spark ignition or diesel engines.

2. Methodology

2.1. Experimental Setup

The experiments performed in this work were conducted on a single-cylinder research engine consisting of a 4-cylinder production GM engine head, with one cylinder fully instrumented and mounted on an FEV engine block. The remaining three cylinders were

deactivated. The piston has a shallow toroidal bowl geometry and the injector included angle is 150 degrees. Details on the engine geometry and valve timing are shown in Table 1.

Table 1. Engine geometry and valve timings.

Engine Displacement	**[cc]**	**423**
Compression Ratio	[-]	16.0
Stroke	[mm]	80.1
Bore	[mm]	82.0
Connecting Rod Length	[mm]	152.4
IVO	[deg aTDC]	360
IVC	[deg aTDC]	−150
EVO	[deg aTDC]	145
EVC	[deg aTDC]	360

A diesel common rail fuel system with a Bosch CP3 pump and a Delphi solenoid-style injector was used. The fuel studied in this work, wet ethanol 80, has a lower lubricity than diesel. Therefore, a lubricity additive (Infineum R655) was blended at a concentration of ~0.05% mass. Previous work with wet ethanol 80 showed that lubricity additive at this concentration did not have an appreciable effect on kinetically-controlled combustion [21].

Data acquisition and engine control were handled using a custom-built LabVIEW code. Low-speed data acquisition of pressure, temperature, flowrates, and emissions data were recorded at 1 Hz. A Horiba MEXA 7100-DEGR measured 5-gas emissions in the exhaust and CO_2 concentration in the intake. The flame ionization detector that measures unburned hydrocarbon (uHC) concentration has a reduced sensitivity to oxygenated organic species. As a result, the measured unburned hydrocarbons are corrected by multiplying by a factor of 1.25 [33]. A Kistler encoder mounted on the crankshaft was used to synchronize crank-angle-resolved measurements of the cylinder, intake manifold, exhaust manifold, and common rail pressure with a resolution of 0.1 degrees. An image of the test cell is shown in Figure 1.

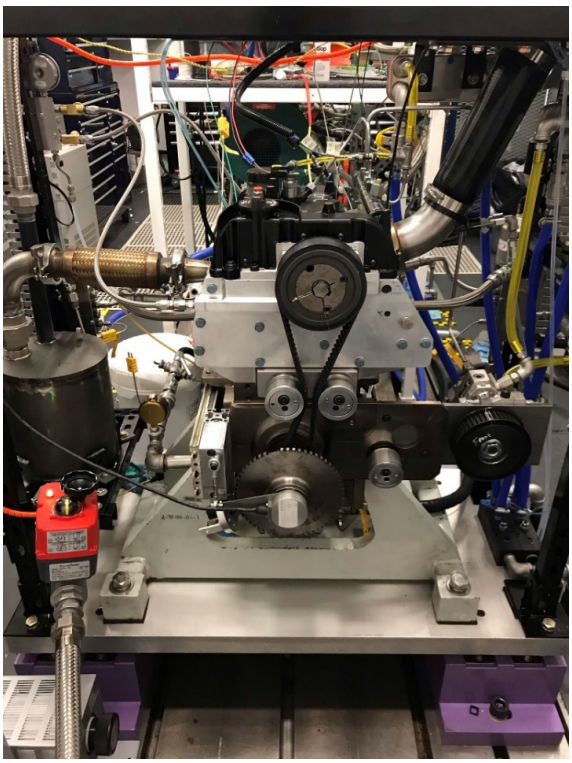

Figure 1. Experimental test cell.

At each operating condition, 300 consecutive cycles were recorded in steady-state operation. A custom MATLAB code was used to process the data, including a statistical-based uncertainty analysis [34]. This uncertainty analysis propagates uncertainty with a confidence interval of 95% using the following equation at each step of data processing:

$$\sigma_z^2 = \sum_{i=1}^{n} \partial z_{x_i}^2 \sigma_{x_i}^2 + 2 \sum_{i=1}^{n-1} \sum_{j=i+1}^{n} \partial z_{x_i} \partial z_{x_j} \sigma_{x_i x_j} + \sigma_{z,meas}^2 + \sigma_{z,instr}^2 \quad (1)$$

where ∂z_{x_i} is the *sensitivity coefficient* of z to x_i (which is the partial derivative of z with respect to x_i), $\sigma_{z,meas}$ is the measurement uncertainty of z, and $\sigma_{z,instr}$ is the instrument uncertainty of z. The uncertainty of parameters related to crank-angle-resolved data, such as CA50 (crank angle location of 50% mass fraction burned), are calculated for each individual cycle and then are reported on a 300-cycle average, since it is the "uncertainty in the next 300 cycles" that is of interest.

The following set of equations define performance parameters used in this work:

- The net fuel conversion efficiency (*NFCE*) is defined as the work output of the cycle divided by the total fuel energy input, given by the following equation:

$$NFCE = \frac{\int_{-360}^{360} PdV}{m_{fuel} Q_{LHV}} \quad (2)$$

- The gross fuel conversion efficiency (*GFCE*) is defined as the work output of the compression and expansion strokes divided by the total fuel energy input, given by the following equation:

$$GFCE = \frac{\int_{-180}^{180} PdV}{m_{fuel} Q_{LHV}} \quad (3)$$

- The combustion efficiency is defined as the total fuel heat release divided by the total fuel energy input, calculated using measurements from the emissions analyzer and given by the following equation:

$$Comb.\ Eff. = 1 - \frac{\sum m_i\ Q_{LHV,\ i}}{m_{fuel} Q_{LHV}} \quad (4)$$

where m_i and $Q_{LHV,\ i}$ are the mass and lower heating value of unburned species, respectively.

- The net or gross thermal efficiencies (N/GTE) are defined as the work output of the either the total cycle or the compression and expansion strokes divided by the total fuel heat release, since the fuel heat release is the energy that is added specifically to the thermodynamic cycle. Therefore, the N/GTE is the $N/GFCE$ divided by the combustion efficiency:

$$N/GTE = \frac{N/GFCE}{Comb\ Eff.} \quad (5)$$

- The indicated specific emissions (*IS*) of a species, x, is defined as the mass flowrate of x in the exhaust divided by indicated power output of the engine:

$$IS\ x = \frac{\dot{m}_x}{Ind.\ Power} \quad (6)$$

These definitions can be found in Heywood [35]. In the following experiments, the engine speed was held constant at 1500 rpm and the common rail pressure was held constant at 1000 bar.

2.2. Thermodynamic Model

A 0-D thermodynamic engine model was used to further understand some of the experimental results shown below. The engine geometry and valve timings in the model are identical to the experimental engine studied. The state of the cylinder is solved at each time step using the specific volume and the specific energy. The specific volume is the volume of the cylinder divided by the mass in the cylinder. The total mass in the cylinder at each time step is found using conservation of mass, accounting for mass flow in and out of the cylinder, which are calculated using the equations of compressible flow through an orifice found in Heywood [35], fuel injection where applicable, and crevice flow. The equations of compressible flow through an orifice are:

$$\dot{m} = \frac{C_D A_R p_0}{\sqrt{RT_0}} \left(\frac{p_T}{p_0}\right)^{1/\gamma} \left\{ \frac{2\gamma}{\gamma - 1} \left[1 - \left(\frac{p_T}{p_0}\right)^{(\gamma-1)/\gamma} \right] \right\}^{1/2} \tag{7}$$

where $\dot{m}$ is the mass flow, C_D is the discharge coefficient, A_R is the area of the orifice, P_0 is the upstream stagnation pressure, R is the universal gas constant divided by the molecular weight of the gas, T_0 is the upstream stagnation temperature, P_T is the throat pressure (assumed to be equal to the downstream pressure), and γ is the ratio of specific heats. When the flow is choked, i.e., when the pressure ratio satisfies:

$$\frac{p_T}{p_0} \leq \left(\frac{2}{\gamma + 1}\right)^{\gamma/(\gamma-1)} \tag{8}$$

Equation (7) can be simplified to:

$$\dot{m} = \frac{C_D A_R p_0}{\sqrt{RT_0}} \sqrt{\gamma} \left(\frac{2}{\gamma + 1}\right)^{(\gamma+1)/2(\gamma-1)} \tag{9}$$

The crevice was modeled as an isothermal constant volume chamber. This is justified due to the very high surface-to-volume ratio of the crevice. The crevice mass flow can be calculated using compressible gas flow equations or with a 0-D approximation, considering the pressure in the crevice volume equals the pressure of the combustion chamber. If the latter assumption is made, the following equation for crevice mass flow can be derived from the ideal gas equation:

$$dm_{cr,i} = \frac{dP_i V_{cr}}{RT_{cr}} \tag{10}$$

where the crevice temperature is some value equal to, or slightly higher than, the wall temperature.

The specific energy is the internal energy of the cylinder divided by the mass in the cylinder. The internal energy is calculated using the first law of thermodynamics for an open system, i.e., conservation of energy, accounting for enthalpy flow from mass transfer, compression and expansion work, heat transfer, evaporative cooling from injected fuel, and heat release from combustion. The crevice heat flow is given by the following equation, consistent with Heywood [35]:

$$\dot{Q}_{cr,\,i} = dm_{cr,i}\left(h_i' - u_i + c_{v,i} T_{Bulk,i}\right) \tag{11}$$

where $dm_{cr,i}$ is the crevice mass flow, u_i is the internal energy of the cylinder gas, and h_i' is the enthalpy of either the cylinder gas, when the crevice mass flow travels from the cylinder to the crevice, or the crevice gas, when the crevice mass flow travels from the crevice to the cylinder. In this work, the heat release from combustion was prescribed by experimental data. Using the thermodynamic state, mixture properties were determined using the ideal gas equation and the NASA polynomials [36], considering a six species gas: Ethanol, O_2, N_2, CO_2, H_2O, and Ar. More information on this thermodynamic model, including validation techniques, are given in Ref. [26].

3. Results

3.1. 10 Bar IMEPn

In a kinetically-controlled combustion strategy, like HCCI, the highest load achievable that is naturally aspirated is limited by a maximum energy release rate or ringing threshold. Ethanol, as a single-stage ignition fuel, does not significantly change reactivity with boost level, meaning that load extension can be achieved through boosting [37]. The high cooling potential of ethanol or wet ethanol also enables stratified kinetically-controlled combustion, where energy release rates are slowed as evaporation-driven thermal stratification increases. Thus, there are two avenues of achieving high load kinetically-controlled combustion with wet ethanol. One clear limitation of the former method is that the peak in-cylinder pressure will rise more rapidly. Additionally, the necessity to keep in-cylinder energy density low will result in low exhaust temperatures that will tax a boost system that already faces a challenge in providing the necessary boost level for engine health. However, the requirement to keep in-cylinder energy density low also results in high thermal efficiency and low thermal NOx production. The introduction of fuel stratification to elongate the heat release process and increase the load without boosting further will increase the global equivalence ratio, which is detrimental to efficiency, and produces regions in the cylinder of high thermal NOx forming potential. EGR can be added to the cylinder to help decrease thermal NOx formation, but this can also be detrimental to efficiency.

To illustrate the tradeoffs that exist here, four cases were compared, one HCCI case and three stratified cases, whose operating conditions are outlined in Table 2. The four cases studied have a load of 10 bar IMEPn and the back pressure was set such that the simulated turbocharger efficiency is 50%, assuming a compressor efficiency of 70%. Indicated performance and emissions results of these four cases are shown in Table 3. In this work, the intake and exhaust pressures were reported on an absolute basis. A brief description of the four cases is as follows:

- Case 1: An HCCI case with an intake pressure of 1.92 bar, such that HCCI combustion could be achieved with a maximum pressure rise rate below 10 bar/deg;
- Case 2: A stratified case where 20% of the fuel is now injected during the compression stroke to elongate the combustion process. The intake pressure is set to 1.65 bar to achieve a similar MPRR as Case 1 with a slightly lower EGR level;
- Case 3: Similar operating conditions to Case 2 with an increase in EGR to reduce NOx emissions;
- Case 4: Identical injection strategy to Case 2 and Case 3, where EGR and boost level are tuned to achieve similar engine-out NOx emissions as Case 1.

In Case 1, where a single injection at −350 deg aTDC is used, lean, premixed operation results in low engine-out NOx, with an IS NOx of 0.2 g/kWh. In Case 2, as expected, the NOx production increased significantly to 1.4 g/kWh. The net fuel conversion efficiency of Case 1 and Case 2 were roughly identical, though they achieved this differently. Being richer, the combustion efficiency of Case 2 was ~0.4 percentage points higher than Case 1, since the higher cylinder energy content of Case 2 increased the effectiveness of sequential autoignition. However, a richer charge and hotter in-cylinder temperatures both have a negative impact on the thermal efficiency of the cycle. The gross thermal efficiency of Case 2 was ~1.4 percentage points lower than Case 1. While this is significant, the lower exhaust enthalpy and higher boost requirement of Case 1 results in significantly more pumping losses than Case 2, ultimately lowering the difference in the net thermal efficiency of the two cases to 0.2 percentage points in favor of Case 1. The exhaust pressure is nearly 0.5 bar higher for Case 1 than it is for Case 2, which puts increased strain on the exhaust system to seal properly as load increases. It should be noted that the assumption of a constant turbocharger efficiency of 50% has a significant impact on this analysis since the difference in pumping losses between the two cases is large.

Table 2. Intake and exhaust pressure (absolute), start of injection (SOI) 1 and SOI 2, and exhaust gas recirculation (EGR) of a four-case comparison.

		Case 1	Case 2	Case 3	Case 4
Intake Pressure	[bar]	1.92 ± 0.02	1.66 ± 0.02	1.67 ± 0.02	1.80 ± 0.02
Exhaust Pressure	[bar]	2.36 ± 0.03	1.88 ± 0.03	1.89 ± 0.03	2.18 ± 0.03
SOI 1	[deg aTDC]	−350	−350	−350	−350
SOI 2	[deg aTDC]	N/A	−60	−60	−60
EGR	[%]	11.6 ± 1.1	7.5 ± 0.9	26.7 ± 0.8	14.5 ± 1.0

Table 3. Indicated performance and emissions results of a four-case study.

		Case 1	Case 2	Case 3	Case 4
NFCE	[%]	44.0 ± 0.6	44.1 ± 0.6	43.4 ± 0.6	43.4 ± 0.6
GFCE	[%]	46.3 ± 0.6	45.4 ± 0.6	44.6 ± 0.6	45.4 ± 0.5
NTE	[%]	47.0 ± 0.6	46.8 ± 0.6	46.3 ± 0.7	46.5 ± 0.6
GTE	[%]	49.5 ± 0.6	48.1 ± 0.6	47.6 ± 0.7	48.7 ± 0.6
Comb. Eff.	[%]	94.6 ± 0.2	95.0 ± 0.1	95.1 ± 0.1	94.6 ± 0.1
IS CO	[g/kWh]	4.9 ± 0.2	4.1 ± 0.2	3.7 ± 0.3	4.6 ± 0.2
IS uHC	[g/kWh]	7.8 ± 0.3	7.3 ± 0.3	6.6 ± 0.2	7.9 ± 0.3
IS NOx	[g/kWh]	0.2 ± 0.01	1.4 ± 0.2	0.5 ± 0.1	0.2 ± 0.02
CA50	[deg aTDC]	11.6 ± 0.1	10.6 ± 0.1	12.6 ± 0.1	12.5 ± 0.1
10–90 BD	[degrees]	8.7 ± 0.1	7.6 ± 0.1	11.7 ± 0.1	11.5 ± 0.1
MPRR	[bar/deg]	9.4	10.8	6.1	6.7

The engine-out NOx of Case 2 can be reduced by increasing the EGR rate and slightly retarding the combustion phasing without changing the boost level of the engine, as shown in Case 3. The increase in EGR also increases the engine-out combustion efficiency. Compared to Case 2, Case 3 has roughly the same pumping losses. The 0.6 percentage point decrease in fuel conversion efficiency is due to two thermodynamic causes. The first is that the increase in EGR rate decreases the ratio of specific heats, which negatively impacts the thermodynamic efficiency (though there is some efficiency benefit to EGR related to lowering peak in-cylinder temperatures, which reduces heat transfer losses). The second is that for Case 3, combustion is phased slightly later and the burn duration is longer than Case 2, both of which decrease the thermodynamic efficiency. The reason combustion is phased slightly later will be explained at the end of this section.

Case 4 raises the boost level to 1.8 bar to strike a balance between boosting, EGR addition, and combustion phasing to produce similar NOx emissions to Case 1. In doing so, the criteria pollutant emissions of Case 4 roughly equal Case 1. There is a 0.6 percentage point decrease in net fuel conversion efficiency as a tradeoff for an increase in specific exhaust enthalpy and a decrease in required boost level. While the exhaust temperature of Case 4 is only 15 K hotter than Case 1, the lower pressure ratio of the turbine of Case 4 means that the temperature drop through the turbine will also decrease, which is favorable for a post-turbine after-treatment system.

Overall, these four cases show that there is flexibility in the operating strategy of a kinetically-controlled combustion strategy with wet ethanol as the fuel (or a fuel with similar fuel properties, like methanol, [38]). Depending on the relative weights given to minimizing criteria emissions and maximizing efficiency, or to the ability and limits of the available engine system hardware, an operating strategy can be defined.

One final digression to be made here is that, during experimental operation, it was found that when EGR was increased from Case 2 to Case 3, a combustion destabilizing dynamic emerged. For all four cases, combustion phasing was controlled by adjusting the intake temperature. As mentioned, for Case 3, combustion was phased slightly later than Case 2. This is because when combustion was phased slightly earlier to match Case 2, a runaway advancement of combustion phasing ensued into a region of engine-damaging heat release rates. In other words, there is an instability in CA50 when CA50

is ~10.5 deg aTDC with the EGR level of Case 3 and Case 4 that prevents steady-state operation here; CA50 will either advance or retard to achieve stability. Practically, this instability is easily stabilized by using well-established combustion phasing control knobs for stratified, kinetically-controlled combustion with wet ethanol: cycle-to-cycle variation of intake stroke injection timing or split fraction. This can be performed with no significant increase in the coefficient of variation (COV) of IMEPn. However, the destabilization made achieving healthy steady-state operation for recording data extremely difficult. While it is not possible to say for certain what causes this behavior, it is highly likely that the destabilization with higher EGR was a result of certain reactivity-enhancing species in the exhaust gas, since it occurs during high EGR operation. Unlike hydrocarbons that exhibit cool flame reactivity, the reactivity of ethanol is not significantly reduced due to a decrease in oxygen concentration from EGR. Rather, there can be a reactivity enhancement due to trace species in the exhaust [39]. In the current situation, one potential candidate is NOx, since the runaway advancement of combustion phasing produces an increasing amount of NOx, creating a positive feedback; chemical kinetics work is required to confirm whether this correlation is the cause of this positive feedback.

3.2. 16 Bar IMEPn

Since wet ethanol has no cool flame reactivity to help stabilize the combustion process as combustion phasing retards, cycle-to-cycle variability of the heat release process begins to increase [40]. While the COV of IMEPn does not increase significantly, the cycle-to-cycle variability of CA50 increases, and as a result, the cycle-to-cycle variability in the peak pressure increases. This behavior results in an average pressure that may stay below the peak pressure limit of the engine, but with many individual cycles far exceeding the peak pressure limit. This is illustrated in Figure 2, where the target peak pressure limit of the engine is defined as 150 bar. The peak pressure limit of 150 bar was selected including a factor of safety since this is a custom research setup; most production diesel engines would be able to reach higher peak pressures, which would expand the operating range of wet ethanol ACI. For now, a mechanism to stabilize the heat release process is required to increase the robustness of combustion. One such mechanism is to add a small amount of fuel to the cylinder after top dead center. This post-style injection will result in a mixing-controlled heat release process that will prevent individual cycles from experiencing very late phased combustion or partial misfires. In doing so, it will eliminate the following rebound cycles, where the heat release process phases very early and the peak cylinder pressure increases significantly. By removing ~15% of the fuel energy from the kinetically-controlled injections and moving it to a mixing-controlled injection at 5 deg aTDC, the COV of peak pressure is reduced from 7% to 2%. The variation in the crank angle location of peak pressure also decreases. Figure 3 illustrates this.

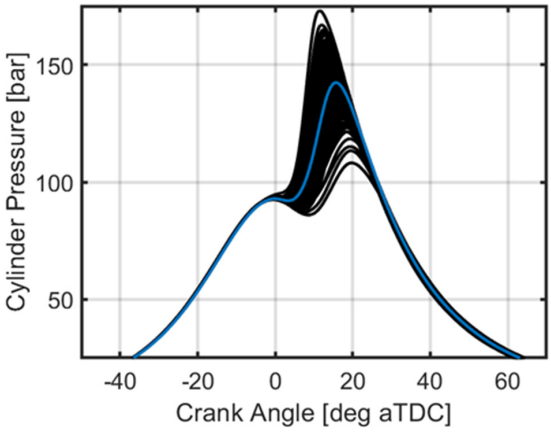

Figure 2. Cylinder pressure vs. crank angle of 300 individual cycles (black) and the average of 300 cycles (blue) for a purely kinetically-controlled combustion case.

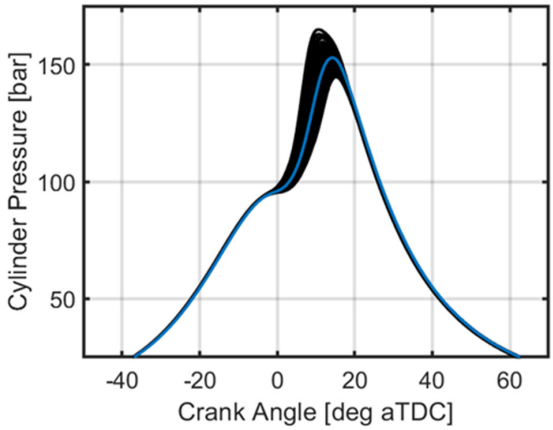

Figure 3. Cylinder pressure vs. crank angle of 300 individual cycles (black) and the average of 300 cycles (blue) for a case where 15% of the fuel is moved from kinetically-controlled injections to a mixing-controlled injection, reducing cyclic variability in the peak pressure.

The combustion stabilization imparted by a mixing-controlled injection of fuel is critical to continuing to push the power density of wet ethanol compression ignition. Therefore, it is worth studying what the impact of injection timing, EGR, and the fraction of fuel energy contained in the mixing-controlled injection are.

3.2.1. Mixing-Controlled Injection Timing Sweep

In this subsection, the results of an injection timing sweep of the mixing-controlled injection (i.e., the "third" injection) is presented, maintaining a constant mixing-controlled fuel energy fraction of 10%. The other 90% is injected through two kinetically-controlled injections at −350 and −60 deg aTDC, with a 75%/25% split (i.e., 67.5% of the fuel is injected during the intake stroke, 22.5% of the fuel is injected during the compression stroke, and the final 10% of the fuel is injected in the mixing-controlled post injection). The intake temperature is adjusted to maintain a constant CA50 of 8.5 deg aTDC. The intake pressure and total fuel injected are constant at 2.0 bar ± 0.05 and 49.3 ± 0.7 mg/cycle, respectively. Figure 4 shows the cylinder pressure and gross heat release rate traces of a subset of four cases from this sweep, with SOI3s of 25, 15, 5, and 0 deg aTDC. In this figure, and other similar figures throughout this work, the gross heat release rate is shown below the cylinder pressure trace. There is no appreciable difference in the cylinder pressure or heat release rate before the mixing-controlled injection when SOI3 is 25 or 15 deg aTDC. The kinetically-controlled heat release process concludes before the ignition of the mixing-controlled injected fuel, which causes SOI3 to have its own separate heat release process. With an SOI3 of 5 deg aTDC, the mixing-controlled heat release process merges into the kinetically-controlled heat release process, but begins after the peak heat release rate, meaning the magnitude of the peak heat release rate is unaffected by the mixing-controlled injection. Finally, with an SOI3 of 0 deg aTDC, the mixing-controlled heat release process begins in the early part of the kinetically-controlled heat release process, resulting in an increase in the peak heat release.

Figure 5, which plots the peak heat release rate and maximum pressure rise rate vs. SOI3, shows that when SOI3 advances early enough to impact the peak heat release rate, it results in an increase in the maximum pressure rise rate. For engine health, the combustion phasing would have to retard to keep the maximum pressure rise rate below some threshold value, such as 10 bar/deg, which would be detrimental to efficiency. Figure 6, which plots the indicated specific emissions of uHC, CO, and NOx vs. SOI3, shows that NOx generally increases with an advancing SOI3. While it seems intuitive that an increase in the peak heat release rate would result in an increase in NOx, NOx increases even before the peak heat release rate is affected. The mixing-controlled heat release process produces NOx on its own due to locally near-stoichiometric combustion, but as SOI3 is phased earlier, the

mixing-controlled heat release process also maintains in-cylinder temperatures above the significant thermal-NOx production threshold for longer (~1700–1800 K). This is illustrated in Figure 7, which plots average in-cylinder temperature vs. crank angle for a subset of the SOI3 sweep.

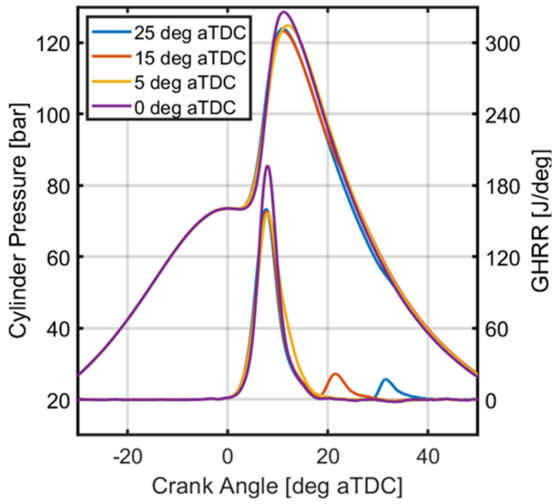

Figure 4. Cylinder pressure and gross heat release rate (GHRR) vs. crank angle for a subset of mixing-controlled injection timing sweep. The legend indicates the mixing-controlled start of injection (SOI3) timing, which contains 10% of the total injected fuel energy.

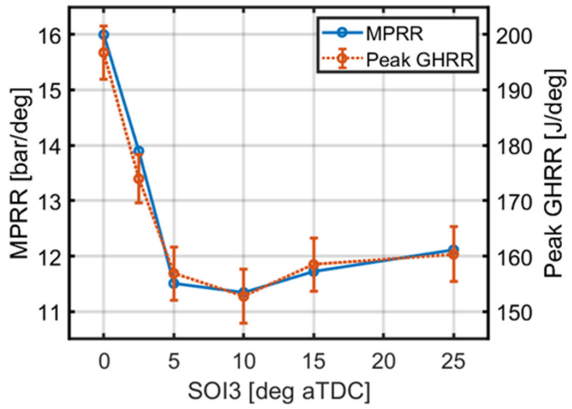

Figure 5. Maximum pressure rise rate (MPRR) and peak gross heat release rate (GHRR) vs. mixing-controlled start of injection (SOI3) timing.

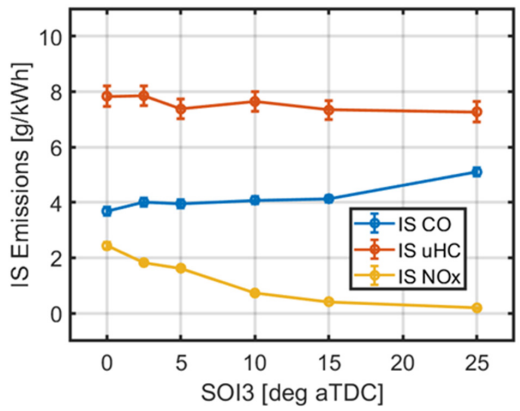

Figure 6. Indicated specific emissions of CO (IS CO), IS uHC, and IS NOx vs. mixing-controlled start of injection (SOI3) timing.

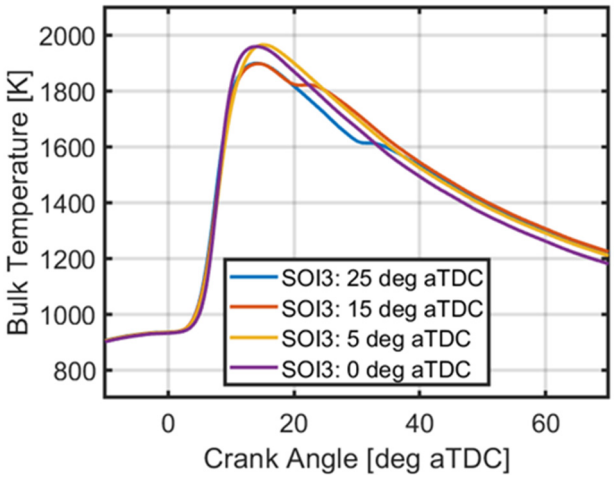

Figure 7. Bulk temperature vs. crank angle for a subset of mixing-controlled injection timing sweep. The legend indicates the mixing-controlled start of injection (SOI3) timing. The significant thermal NOx production threshold is ~1700–1800 K.

3.2.2. External, Cooled Exhaust Gas Recirculation Sweep

Next, an external, cooled EGR sweep was performed to study the impact on NOx emissions and other performance parameters of the triple injection strategy with wet ethanol 80. The load and intake pressure remained constant at 16.0 ± 0.05 bar and 2.65 ± 0.05 bar, respectively, with the exhaust pressure set such that the turbocharger efficiency is 50%. SOI1, SOI2, and SOI3 remained constant at −350, −60, and 5 deg aTDC, respectively. The intake temperature was adjusted to maintain a constant CA50 of 10.5 ± 0.2 deg aTDC. Operating conditions that were not held constant across the sweep are shown in Table 4.

Table 4. Operating conditions of EGR sweep.

EGR	**[%]**	**0.0%**	**15.8%**	**28.5%**	**37.1%**
Fuel Split SOI1/2/3	[%/%/%]	50/35/15	50/35/15	60/25/15	65/20/15
Total Fuel	[mg/cyc]	90.5 ± 1.0	89.8 ± 1.1	89.9 ± 1.0	92.8 ± 1.0
Equivalence Ratio	[-]	0.54 ± 0.01	0.64 ± 0.01	0.80 ± 0.01	0.95 ± 0.01
Intake Temp.	[K]	378.8 ± 2.2	383.9 ± 2.2	393.5 ± 2.2	398.8 ± 2.2

Figure 8 shows the net fuel conversion, net thermal, and engine-out combustion efficiency vs. EGR. The net thermal efficiency increases slightly as EGR is increased from 0% to 15.8%, and then decreases slightly as EGR increases further. The combustion efficiency increases slightly as EGR fraction increases from 0% to 28.5% and then experiences a decrease as EGR increases further to 37.1%. This decrease in combustion efficiency is due to a sharp increase in IS CO emissions, shown in Figure 9, which plots IS uHC, IS CO, and IS NOx vs. EGR. The CO emissions increase because the global equivalence ratio is 0.95. With a nearly stoichiometric equivalence ratio and a fuel-stratified combustion chamber, fuel in locally rich areas cannot proceed from CO to CO_2 due to oxygen deprivation before CO conversion chemistry freezes due to expansion. Overall, the net fuel conversion efficiency is roughly constant as EGR increases from 0% to 28.5% and then decreases ~1 percentage point as EGR increases further to 37.1%. While 37.1% EGR can result in an engine-out IS NOx of 0.06 g/kWh, a respectable 0.2 g/kWh engine-out IS NOx can be achieved with 28.5% EGR without an efficiency penalty.

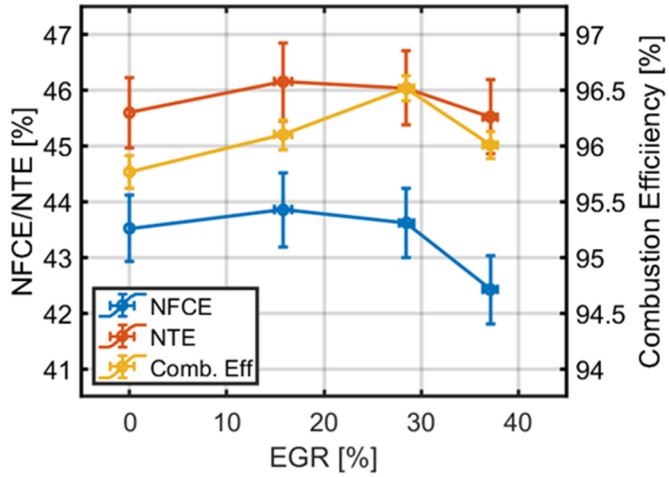

Figure 8. Net fuel conversion (FC) efficiency, net thermal efficiency, and combustion efficiency vs. external, cooled exhaust gas recirculation (EGR).

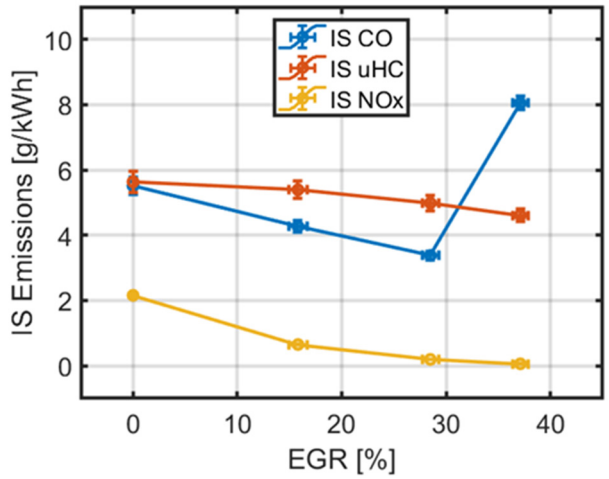

Figure 9. Indicated specific emissions of CO (IS CO), IS uHC, and IS NOx vs. external, cooled exhaust gas recirculation (EGR).

3.3. Mixing-Controlled Fuel Fraction Sweep

In this subsection, the study of the split of fuel energy that is contained in the mixing-controlled vs. kinetically-controlled injections is presented. This was performed by starting with a purely kinetically-controlled combustion case and moving fuel from kinetically-controlled injections to mixing-controlled injections. The kinetically-controlled injections are the fully premixed injection at −350 deg aTDC and the partially premixed injection at −60 deg aTDC. For the mixing-controlled injections, the injection timing and split fraction was chosen based on a brief optimization routine, though a more robust study could yield better performance. The injection timing and injected fuel amount in each injection is shown in Table 5. The estimation of individual injected fuel amounts is determined from a correlation between commanded injection duration and mass of wet ethanol injected at 1000 bar common rail pressure developed experimentally on the engine in this study. This estimation provides reasonable accuracy, though the interaction between injections via changes in rail pressure is not captured. Therefore, the reported split fractions between injections will carry some uncertainty. The intake pressure remained constant at 2 bar and the exhaust pressure was adjusted to maintain a constant turbocharger efficiency of 50%.

Table 5. Injection parameters for kinetically-controlled (KC) and mixing-controlled (MC) injections for the MC fraction sweep. * The injection at −30 deg aTDC behaves kinetically, but functions as a pilot injection, which is typical for MC combustion.

Total Fuel Mass		**[mg/cyc]**	**52.9 ± 0.7**	**52.2 ± 0.7**	**51.8 ± 0.7**	**51.2 ± 0.7**	**51.8 ± 0.7**
MC Fraction		**[%]**	**0**	**22**	**45**	**70**	**100 ***
KC	SOI 1	[deg aTDC]	−350	−350	−350	−350	–
		[mg/cyc]	39.6	29.1	21.5	15.4	–
	SOI 2	[deg aTDC]	−60	−60	−60	–	−30
		[mg/cyc]	13.3	11.6	7.0	–	11.2
MC	SOI 1	[deg aTDC]	–	–	–	−11	−15
		[mg/cyc]	–	–	–	4.5	6.5
	SOI 2	[deg aTDC]	–	6	−2	−3	2
		[mg/cyc]	–	11.5	23.3	31.3	34.1

Figure 10 shows the cylinder pressure and gross heat release rate traces of each case in the mixing-controlled fraction sweep. The first thing to notice is that the compression pressure increases as mixing-controlled fraction increases. This is because as fuel is removed from the kinetically-controlled injections, the ratio of specific heats during the compression process increases and there is less evaporative cooling during the compression stroke before TDC. Instead, some of the evaporative cooling is transitioned to after TDC during the mixing-controlled injection. As the mixing-controlled fraction increases, the heat release rate profile transforms from a traditional Gaussian-style, HCCI-like heat release profile to a traditional mixing-controlled-style heat release profile. Because wet ethanol has a high autoignition resistance and cooling potential, which result in long ignition delays, a significant amount of heat release is required from the pilot injection to ignite the main injection of wet ethanol during high mixing-controlled fraction operation. This creates an efficiency tradeoff where it would be beneficial to advance the main injection for more favorable combustion phasing but would require an advancement of the pilot injection to phase the pilot heat release earlier, which is detrimental to efficiency.

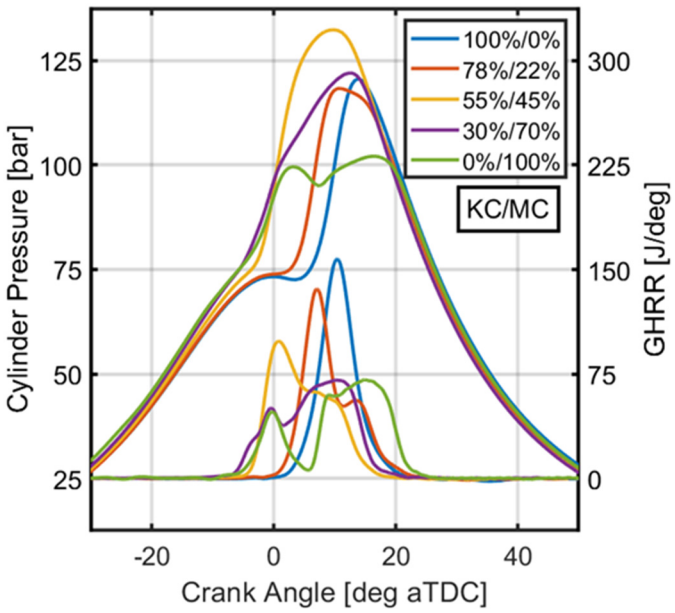

Figure 10. Cylinder pressure and gross heat release rate (GHRR) of a mixing-controlled fraction sweep. The legend indicates the fuel energy split between kinetically-controlled (KC) and mixing-controlled (MC) injections.

The net fuel conversion efficiency, net thermal efficiency, and engine-out combustion efficiency are all plotted vs. mixing-controlled fraction in Figure 11. The corresponding indicated specific emissions are shown in Figure 12. There is a clear upward trend in combustion efficiency with an increase in mixing-controlled fraction associated with a strong decrease in CO and uHC emissions. NOx emissions increase with increasing mixing-controlled fraction and a clear downward trend in net thermal efficiency with mixing-controlled fraction is present. There is a less severe, but still clear downward trend in net fuel conversion efficiency. The increasing trend in combustion efficiency is not surprising, since it is well-established that the combustion efficiency of mixing-controlled combustion is >99% as long as the global equivalence ratio is sufficiently lean and the ignition delay is reasonably short, both of which conditions are satisfied here. The decrease in thermal efficiency is in part due to an elongation of the main heat release process as well as a significant increase in the amount of heat released near or before TDC. However, another factor that is significantly detrimental to the thermal efficiency of the thermodynamic cycle is the heat removal due to the high cooling potential of the fuel, which will be investigated with thermodynamic modeling below.

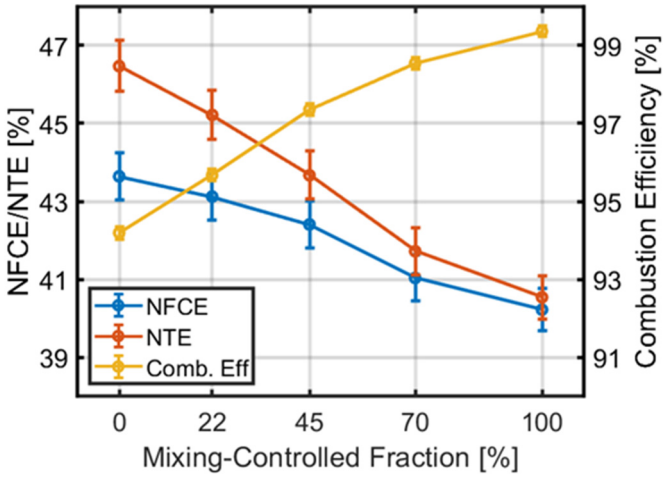

Figure 11. Net fuel conversion (FC) efficiency, net thermal efficiency, and combustion efficiency vs. mixing-controlled fraction.

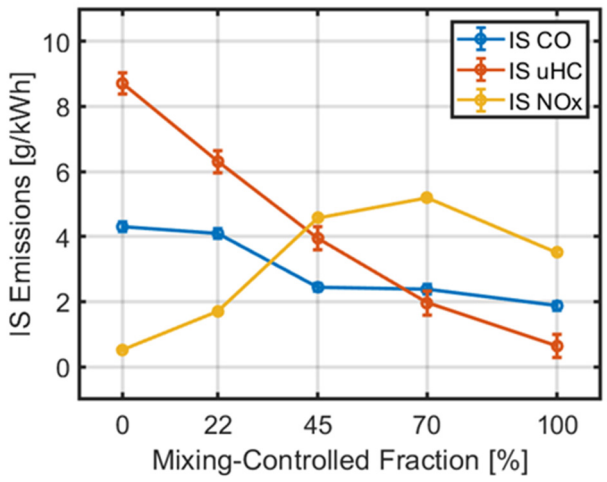

Figure 12. Indicated specific emissions of CO (IS CO), IS uHC, and IS NOx vs. mixing-controlled fraction.

The heat removal from the evaporation and heating of injected fuel is an important fact about wet ethanol in compression ignition. In order to shed more light on this, a 0-D thermodynamic model will be briefly used. Experimentally measured boundary conditions,

such as the intake and exhaust states, initialize the model. The injection parameters and experimentally determined gross heat release rate (GHRR) are also inputs. Validation of the model was performed at all five operating conditions in the mixing-controlled fraction sweep; Figure 13 shows validation of the model at the second operating point, 78/22 KC/MC.

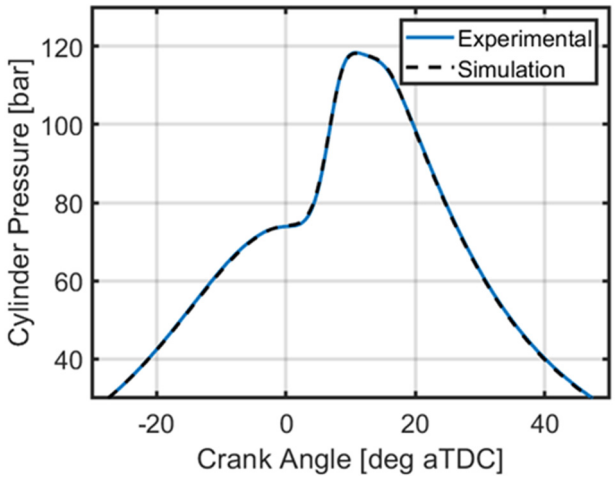

Figure 13. Cylinder pressure vs. crank angle of showing validation of 0-D thermodynamic engine cycle.

After validating the model, the individual contributions of the heat of vaporization among other factors can be explored thermodynamically. To simulate the effect of the heat of vaporization of the mixing-controlled injection on the thermodynamic cycle, a back-to-back comparison is performed, where the heat of vaporization of the fuel is artificially set to 0 in the model. If the heat of vaporization of the operating condition in Figure 13 (i.e., the second operating point, 78/22 KC/MC) is artificially set to zero in the simulation, there is no evaporation-driven heat removal from the cycle and the net fuel conversion efficiency increases by 0.8 percentage points compared to the case with the realistic heat of vaporization of this fuel. Since the gross heat release rate was not changed, the combustion efficiency of the simulation is unchanged. Therefore, this change in net fuel conversion efficiency is equivalent to, and more representative experimentally, of a change in the net thermal efficiency. If the heat of vaporization is set to zero in the simulation for the pure mixing-controlled case, a 2.1 percentage increase in the net fuel conversion efficiency is observed compared to the case with a realistic heat of vaporization.

A separate thermodynamic factor that can be explored with the thermodynamic model is the fuel's temperature as it enters the cylinder. In the model, the fuel temperature, which defines the fuel's enthalpy as the fuel enters the 0-D control volume during injection, is 400 K. With mixing-controlled timings, this temperature is much lower than the bulk gas temperature. Some energy from the gases in the cylinder is absorbed by the incoming fuel to heat the fuel as it is injected, evaporates, and forms a gaseous mixture with the air (and potentially fuel) that is already in the cylinder. The thermodynamic model can be used to explore how this incoming fuel temperature affects the thermodynamics of the cycle by changing the fuel temperature and examining the differences in thermal efficiency. If the fuel temperature is raised from 400 K to 800 K in the model, there is a 1.6 percentage point increase in fuel conversion efficiency compared to the baseline pure mixing-controlled case. If the heat of vaporization is set to zero and the fuel temperature is set to 800 K, a 3.6 percentage point increase in fuel conversion efficiency is seen compared to the baseline. This is summarized in Figure 14, which shows the cylinder pressure vs. crank angle of the four simulations.

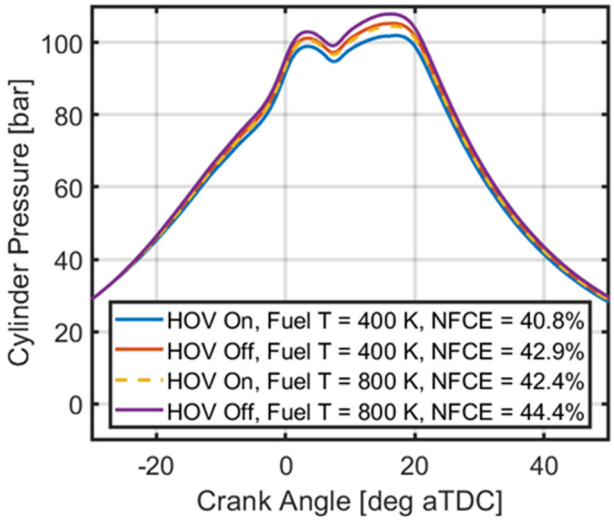

Figure 14. Cylinder pressure vs. crank angle for four simulated mixing-controlled cases. The legend indicates whether the heat of vaporization (HOV) is on or off ("on" meaning that the actual HOV of wet ethanol 80 is used, and "off" meaning that the HOV was artificially set to zero) in the model, the fuel temperature at injection, and the net fuel conversion efficiency (NFCE).

It is important to note that simulations of the injection event in a 0-D model are not perfectly exact. The injection profile of the fuel in the model is a square wave. The starts of injection are set as the experimental starts of injection timings with a two-crank angle offset to account for the opening of the injector. In this 0-D model, once the fuel is injected, evaporative cooling occurs instantaneously, and the fuel is assumed to be well-mixed in the control volume. Of course, this is not physical, but it is a limitation of 0-D modeling. This inexactness is more pronounced with the heating of the injected fuel. The heating of the fuel is complex since both the heating timescale and the amount of heat absorption are unclear. Therefore, these results should be taken as a trend-wise demonstration of the importance of HOV and fuel heating near TDC associated with a mixing-controlled injection when using wet ethanol 80 or any other high cooling potential fuel.

What these thermodynamic modeling results demonstrate is that the heat absorption of wet ethanol upon injection has a significant impact on the efficiency of the thermodynamic cycle. The heat of vaporization of wet ethanol 80 is ~6% of its lower heating value, which is roughly a factor of ten higher than diesel. A high specific heat also means the total heat absorption is likely higher than 6%. For kinetically-controlled injections, the heat removal does not occur at a time during the thermodynamic cycle where heat removal is significantly detrimental to efficiency, i.e., far from firing TDC. However, for mixing-controlled injections, this heat removal occurs near firing TDC and always somewhat precedes heat release. At the very least, the heat removal from evaporation removes 6% of the total heat release from the cylinder. With thermal efficiency on the order of 50%, that means that pure mixing-controlled compression ignition of wet ethanol 80 incurs roughly a 3-percentage-point reduction of thermal efficiency compared to kinetically-controlled strategies. This is in agreement with an experimental result in the literature, where methanol-fueled mixing-controlled compression ignition displayed a lower fuel conversion efficiency than diesel-fueled mixing-controlled compression ignition despite having a more thermodynamically favorable heat release process [41].

While mixing-controlled combustion of wet ethanol 80 results in higher combustion efficiency than kinetically-controlled combustion, these results present a clear thermodynamic penalty to the evaporation of a high cooling potential fuel in a mixing-controlled strategy. From an emissions perspective, there is a NOx-combustion efficiency tradeoff. However, NOx emissions regulations are the biggest hurdle for future internal combustion engines. Therefore, it may be advantageous to use kinetically-controlled combustion of

wet ethanol 80 compared to mixing-controlled combustion of wet ethanol 80, which would favor lower NOx emissions at the expense of higher CO and uHC emissions. An additional advantage of kinetically-controlled combustion of wet ethanol 80 over mixing-controlled combustion is that higher CO and uHC emissions result in more available energy in the exhaust in the form of partially oxidized fuel, which then reacts exothermically in a catalyst to help with low temperature aftertreatment of CO, uHC, and NOx emissions. With this in mind, the optimal injection strategy should minimize the amount of fuel injected in the mixing-controlled injections, only using as much as is required for combustion stabilization at high loads.

3.4. Load Sweep

Previous work with purely kinetically-controlled compression ignition of wet ethanol 80 showed a load extension of up to ~8 bar IMEPn [21]. In this section, a load sweep is performed from 10 bar IMEPn to 22 bar IMEPn using a triple injection strategy where injection timing and duration, EGR, and boost level are simultaneously optimized to maintain either a peak pressure limit of ~150 bar or a maximum pressure rise rate of 10 bar/deg, while minimizing NOx emissions without incurring significant efficiency penalties. Figure 15, which plots intake pressure and peak cylinder pressure vs. IMEPn, shows that, in the first half of the load sweep to 16 bar IMEPn, the intake pressure continues to rise rapidly with load. As the peak pressure limit of the engine approaches, the rate of boost level increase with load reduces dramatically and mixing-controlled injections must be used to increase the load further. Note, this research engine had a peak pressure limit of 150 bar for safety considerations, but most production diesel engines can achieve higher pressures, which would have allowed further minimization of the mixing-controlled fraction and optimization of the efficiency and emissions performance, especially at loads greater than 16 bar.

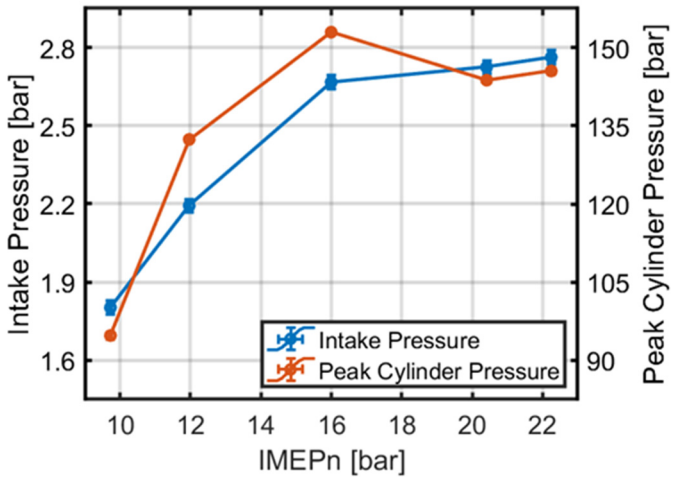

Figure 15. Intake pressure and peak cylinder pressure vs. net indicated mean effective pressure (IMEPn).

Figure 16 plots the net fuel conversion, net thermal, and combustion efficiency vs. IMEPn. As load increases from 12 bar IMEPn, the combustion efficiency increases and the net thermal efficiency decreases as both the mixing-controlled fraction and the specific energy density of the charge increases. There is a thermodynamic penalty to increasing the load without increasing the boost level due to the associated increase in peak temperatures and decrease in the ratio of specific heats. Furthermore, the incorporation of mixing-controlled injections to stabilize the combustion process at high loads, maintaining the peak cylinder pressure limit, incurs a thermodynamic penalty, as discussed above. However, enabling a maximum load of 22 bar IMEPn with a peak cylinder pressure of less than 150 bar with wet ethanol 80 makes this efficiency penalty acceptable. Figure 17, which plots

IS uHC, CO, and NOx vs. IMEPn, shows that, up to 20 bar IMEPn, IS NOx is kept below 0.3 g/kWh. At a peak load of 22 bar, the engine out IS NOx is 1.3 g/kWh with a net fuel conversion efficiency of 42% and a combustion efficiency of 98.7%.

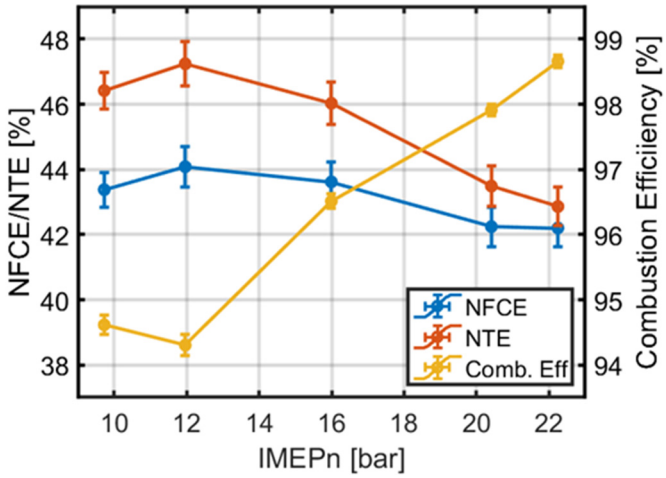

Figure 16. Net fuel conversion (FC) efficiency, net thermal efficiency, and combustion efficiency vs. net indication mean effective pressure (IMEPn).

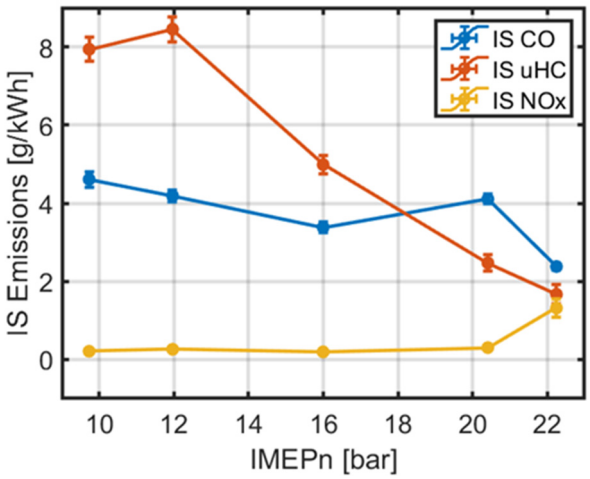

Figure 17. Indicated specific emissions of CO (IS CO), IS uHC, and IS NOx vs. net indication mean effective pressure (IMEPn).

3.5. Discussion: Emissions and Efficiency

Ethanol is a two-carbon oxygenated hydrocarbon, meaning it has a very low soot potential compared to conventional fuels. It is expected that the particulate matter level of wet ethanol 80 would be undetectable using a smoke meter or opacity meter, especially under the globally lean, partially premixed operating conditions studied in this work. Therefore, the authors attempted to use a Cambustion DMS500 to measure the particle size distribution, which is sensitive enough to measure low concentrations of small particles. During globally lean, partially premixed operation at 10 bar IMEPn, all soot concentration measurements were less than ~1.3 mg/m^3, which is a calculated filter smoke number (FSN) of 0.1. Further, no appreciable amount of soot agglomeration was observed, i.e., no large particles. An example of the particle number distribution and the cumulative mass observed is shown in Figure 18.

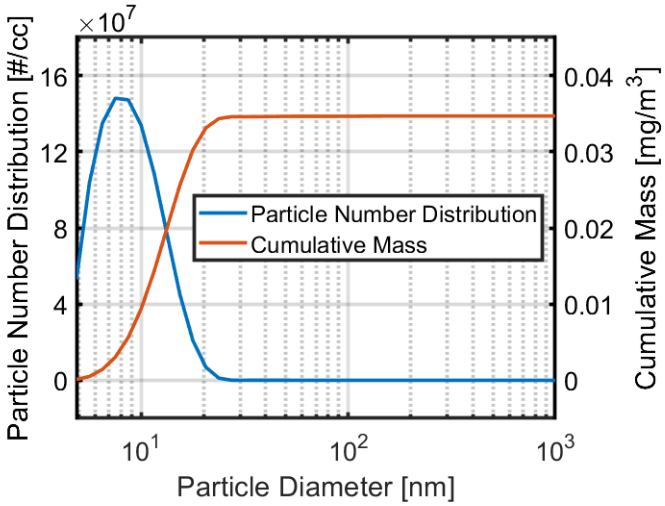

Figure 18. Particle number distribution and cumulative mass vs. particle diameter measured on a DMS 500 under lean, partially premixed operation at 10 bar IMEPn.

Over the course of the experiments, due to the high water content in the exhaust, particularly in operating conditions with high equivalence ratios, the dew point exceeded the temperature in the heated line, causing the flow meters in the DMS500 to fail over time. Thus, a deeper analysis on the particulate distribution, particularly during the mixing-controlled fraction sweep, could not be performed in the current work. Other researchers have successfully measured the particulate matter of neat ethanol in partially premixed combustion, confirming that near-zero particulate matter was produced [42]. Therefore, conclusive measurements of particulate matter with wet ethanol 80 could not be made in this work, but the reliance on kinetically-controlled combustion is expected to result in essentially zero particulate mass as long as the partially premixed injection does not significantly impinge on the walls and piston crown, where there may not be enough time for evaporation before combustion.

The water content in the fuel will also have an impact on the engine-out emissions. As a high cooling potential diluent, the water in the fuel increases the fuel's ignition delay, resulting in more time for fuel-air mixing before ignition. Therefore, there is a lower chance of soot emissions due to the water, even independent of the low carbon number and oxygenation of ethanol. Researchers have noted that water-fuel emulsions using fossil fuels result in lower soot emissions in compression ignition engines [43]. An emulsifier is required with fossil fuels because the water and oil will not mix otherwise, but an emulsifier is not required with the alcohol fuels.

The diluent effect of water will also result in lower NOx emissions, like EGR, particularly for the mixing-controlled phase of combustion since the local water concentration naturally scales with the local fuel concentration. Again, past research with water-fuel emulsions with found lower NOx emissions [43].

The results presented here demonstrate high power-density compression ignition operation on a light-duty production engine geometry, with a piston swap being the only hardware change. Compared to diesel-fueled compression ignition on the same engine with a stock re-entrant bowl piston, the net fuel conversion efficiency of wet ethanol 80 compression ignition using a triple injection strategy is slightly higher and the NOx emissions are significantly lower. ACI can achieve more rapid combustion than diesel combustion without high localized heat transfer rates from the diffusion burn in the piston bowl. However, in ACI, the peak heat release rate occurs a little later in the piston motion than the premixed spike in diesel, which results lower pressure rise rates. Additionally, the minimization of mixing-controlled heat release results in significantly less engine-out NOx emissions, and EGR can be used liberally since there is no soot-NOx tradeoff to consider (since there is no soot). On a system level, wet ethanol 80 will not require a diesel particulate

filter that undergoes regeneration and can shift to regimes with lower engine-out NOx, reducing diesel exhaust fluid consumption in a lean-NOx aftertreatment system. To achieve very high loads, when power density is a priority, mixing-controlled combustion can be used to achieve combustion stability, with a slight efficiency and emissions penalty.

One of the remaining challenges is reducing the level of charge heating required to achieve autoignition of wet ethanol 80. This problem can be solved by increasing the compression ratio of the engine, using uncooled EGR, and/or using thick thermal barrier coatings to retain heat transferred out of the cylinder during combustion and preheat the incoming charge [44,45]. Since wet ethanol 80 has a high cooling potential, overheating the incoming charge is not an issue, since the evaporative cooling of the fuel can be used to control the intake valve closing temperature. These techniques have additional benefits on efficiency and engine-out emissions, presenting a promising opportunity for using a carbon-neutral fuel in a high-efficiency, low engine-out emissions combustion strategy with minimal changes to existing engine hardware.

4. Conclusions

In this work, compression ignition of wet ethanol 80, a domestically sourced and mass-produced biofuel with single stage ignition properties, was studied at high loads under boosted conditions. At 10 bar IMEPn, performance differences between premixed and stratified kinetically-controlled combustion were experimentally studied. At 16 bar IMEPn, the addition of a mixing-controlled injection to stratified kinetically-controlled combustion with wet ethanol 80 was experimentally studied with support from zero-dimensional thermodynamic modeling. Finally, a load sweep was experimentally performed at 1500 rpm. The following conclusions can be drawn:

1. When the air-handling or aftertreatment system are not constrained, the boost level of the engine can increase sufficiently with a load that enables pure HCCI without engine damaging heat release rates with wet ethanol 80. However, the same load can be achieved with a lower and more realistic boost level by injecting some wet ethanol during the compression stroke to elongate the heat release process. This increases the specific enthalpy of the exhaust, which is beneficial for the turbocharging and aftertreatment systems, as well as for lowering pumping losses. While this results in an increase in engine-out NOx, boost level and EGR can be tuned synergistically to reduce engine-out NOx emissions.
2. As the peak pressure limit of the engine approaches and combustion phasing must retard, moving some fraction of the fuel to an injection near TDC to enable a mixing-controlled phase of the heat release process helps stabilize the kinetically-controlled combustion process, decreasing the COV of peak pressure and enabling healthier engine operation at high loads.
3. Due to the high cooling potential of wet ethanol 80, which is ~6% of the lower heating value of the fuel, injections near TDC have a significant thermodynamic penalty due to heat absorption from evaporation and heating of the fuel. As a result, the thermal efficiency decreases as fuel is moved from kinetically-controlled injections to mixing-controlled injections. Injecting diesel fuel near TDC in conventional diesel combustion also causes heat to be absorbed from the thermodynamic cycle at a time that reduces efficiency; however, due to the much lower cooling potential of diesel, this effect is fairly negligible in conventional diesel combustion. With wet ethanol 80 or any other high cooling potential fuel, the efficiency reduction is not negligible.
4. There is also an increase in combustion efficiency (decrease in CO and uHC emissions) and an increase in NOx emissions as fuel is moved from kinetically-controlled injections to mixing-controlled injections.
5. By using wet ethanol 80 in a triple injection strategy, a load of 22 bar IMEPn is achieved with diesel-like (or higher) efficiency, low engine-out NOx emissions, no measurable particulate matter, and while maintaining a peak cylinder pressure below 150 bar.

Overall, these results indicate that high-load operation of wet ethanol 80 fueled compression ignition is possible by combining advanced kinetically-controlled combustion and conventional mixing-controlled combustion. This enables a high-power density and a highly controllable internal combustion engine concept with a low carbon intensity biofuel.

Author Contributions: Conceptualization, B.G. and B.L.; methodology, B.G.; software, B.G.; validation, B.G. and Z.Y.; formal analysis, B.G.; investigation, B.G., Z.Y. and J.G.; resources, B.L.; data curation, B.G. and Z.Y.; writing—original draft preparation, B.G.; writing—review and editing, B.G., Z.Y., J.G. and B.L.; visualization, B.G.; supervision, B.L.; project administration, B.L.; funding acquisition, N/A. All authors have read and agreed to the published version of the manuscript.

Funding: This research received no external funding.

Institutional Review Board Statement: Not applicable.

Informed Consent Statement: Not applicable.

Data Availability Statement: The data presented in this study are available on request from the corresponding author.

Conflicts of Interest: The authors declare no conflict of interest.

References

1. Dees, J.; Goldstein, H.; Grim, G.; Harris, K.; Huang, Z.; Lee, U.; Meyer, P.A.; Rowe, I.; Sanchez, D.; Simon, A.J.; et al. U.S. DRIVE Net-Zero Carbon Fuels Technical Team Analysis Summary Report 2020. USDRIVE; September 2021. Available online: https://www.energy.gov/eere/vehicles/articles/us-drive-net-zero-carbon-fuels-technical-team-analysis-summary-report-2020 (accessed on 21 March 2020).
2. Santos, N.D.S.A.; Roso, V.R.; Malaquias, A.C.T.; Baêta, J.G.C. Internal combustion engines and biofuels: Examining why this robust combination should not be ignored for future sustainable transportation. *Renew. Sustain. Energy Rev.* **2021**, *148*, 111292. [CrossRef]
3. Liu, C.-G.; Xiao, Y.; Xia, X.-X.; Zhao, X.-Q.; Peng, L.; Srinophakun, P.; Bai, F.-W. Cellulosic ethanol production: Progress, challenges and strategies for solutions. *Biotechnol. Adv.* **2019**, *37*, 491–504. [CrossRef] [PubMed]
4. Huo, Y.-X.; Wernick, D.G.; Liao, J. Toward nitrogen neutral biofuel production. *Curr. Opin. Biotechnol.* **2012**, *23*, 406–413. [CrossRef] [PubMed]
5. Perlack, R.D.; Stokes, B.J. *U.S. Billion-Ton Update: Biomass Supply for a Bioenergy and Bioproducts Industry*; Report ORNL/TM-2005/66; Oak Ridge National Laboratory: Oak Ridge, TN, USA, 2011. [CrossRef]
6. Adeniyi, O.M.; Azimov, U.; Burluka, A. Algae biofuel: Current status and future applications. *Renew. Sustain. Energy Rev.* **2018**, *90*, 316–335. [CrossRef]
7. Renewable Fuels Association. *2021 Ethanol Industry Outlook*; Renewable Fuels Association: Ellisville, MO, USA, 2021.
8. Oxenham, L.; Wang, Y. A Study of the Impact of Methanol, Ethanol and the Miller Cycle on a Gasoline Engine. *Energies* **2021**, *14*, 4847. [CrossRef]
9. Szybist, J.P.; Busch, S.; McCormick, R.L.; Pihl, J.A.; Splitter, D.A.; Ratcliff, M.A.; Kolodziej, C.P.; Storey, J.M.; Moses-DeBusk, M.; Vuilleumier, D.; et al. What fuel properties enable higher thermal efficiency in spark-ignited engines? *Prog. Energy Combust. Sci.* **2020**, *82*, 100876. [CrossRef]
10. Flowers, D.L.; Aceves, S.M.; Frias, J.M. *Improving Ethanol Life Cycle Energy Efficiency by Direct Utilization of Wet Ethanol in HCCI Engines*; SAE Technical Paper 2007-01-1867; SAE International: Warrendale, PA, USA, 2007. [CrossRef]
11. Chen, Z.; Deng, J.; Zhen, H.; Wang, C.; Wang, L. Experimental Investigation of Hydrous Ethanol Gasoline on Engine Noise, Cyclic Variations and Combustion Characteristics. *Energies* **2022**, *15*, 1760. [CrossRef]
12. Najt, P.M.; Foster, D.E. *Compression-Ignited Homogeneous Charge Combustion*; SAE Technical Paper 830264; SAE International: Warrendale, PA, USA, 1983. [CrossRef]
13. Mack, J.H.; Aceves, S.; Dibble, R. Demonstrating direct use of wet ethanol in a homogeneous charge compression ignition (HCCI) engine. *Energy* **2009**, *34*, 782–787. [CrossRef]
14. Gohn, J.; Gainey, B.; Zainul, S.; Lawler, B. Wet ethanol in LTC: How water fraction and DTBP affect combustion and intake temperature at naturally aspirated and boosted conditions. *Fuel* **2020**, *267*, 117094. [CrossRef]
15. Telli, G.; Zulian, G.; Lanzanova, T.; Martins, M.; Rocha, L. An experimental study of performance, combustion and emissions characteristics of an ethanol HCCI engine using water injection. *Appl. Therm. Eng.* **2021**, *204*, 118003. [CrossRef]
16. Sjöberg, M.; Dec, J.E. *Smoothing HCCI Heat-Release Rates Using Partial Fuel Stratification with Two-Stage Ignition Fuels*; SAE Technical Paper 2006-01-0629; SAE International: Warrendale, PA, USA, 2006. [CrossRef]
17. Pintor, D.L.; Dec, J.; Gentz, G. *Φ-Sensitivity for LTGC Engines: Understanding the Fundamentals and Tailoring Fuel Blends to Maximize This Property*; SAE Technical Paper 2019-01-0961; SAE International: Warrendale, PA, USA, 2019. [CrossRef]

18. Lopez-Pintor, D.; Dec, J.E. Experimental Evaluation of a Gasoline-like Fuel Blend with High Renewable Content to Simultaneously Increase φ-Sensitivity, RON, and Octane Sensitivity. *Energy Fuels* **2021**, *35*, 16482–16493. [CrossRef]
19. Curran, S.; Dec, J.E.; Fioroni, G.; Kolodziej, C.; Pal, P. Heavy-Duty Advanced Compression Ignition. United States; 2020. Available online: https://www.osti.gov/servlets/purl/1781306 (accessed on 21 March 2020).
20. Zhang, Y.; Sellnau, M. A Computational Investigation of PPCI-Diffusion Combustion Strategy at Full Load in a Light-Duty GCI Engine. *SAE Int. J. Adv. Curr. Pract. Mobil.* **2021**, *3*, 1757–1775. [CrossRef]
21. Gainey, B.; Hariharan, D.; Yan, Z.; Zilg, S.; Boldaji, M.R.; Lawler, B. A split injection of wet ethanol to enable thermally stratified compression ignition. *Int. J. Engine Res.* **2018**, *21*, 1441–1453. [CrossRef]
22. Gainey, B.; Lawler, B. The role of alcohol biofuels in advanced combustion: An analysis. *Fuel* **2020**, *283*, 118915. [CrossRef]
23. Sjoberg, M.; Dec, J.E. Ethanol Autoignition Characteristics and HCCI Performance for Wide Ranges of Engine Speed, Load and Boost. *SAE Int. J. Engines* **2010**, *3*, 84–106. [CrossRef]
24. Sarathy, S.M.; Osswald, P.; Hansen, N.; Kohse-Höinghaus, K. Alcohol combustion chemistry. *Prog. Energy Combust. Sci.* **2014**, *44*, 40–102. [CrossRef]
25. Gainey, B.; Yan, Z.; Gohn, J.; Boldaji, M.R.; Lawler, B. *TSCI with Wet Ethanol: An Investigation of the Effects of Injection Strategy on a Diesel Engine Architecture*; SAE Technical Paper 2019-01-1146; SAE International: Warrendale, PA, USA, 2019. [CrossRef]
26. Gainey, B.; Gohn, J.; Yan, Z.; Malik, K.; Boldaji, M.R.; Lawler, B. *HCCI with Wet Ethanol: Investigating the Charge Cooling Effect of a High Latent Heat of Vaporization Fuel in LTC*; SAE Technical Paper 2019-24-0024; SAE International: Warrendale, PA, USA, 2019. [CrossRef]
27. Boldaji, M.R.; Gainey, B.; O'Donnell, P.; Gohn, J.; Lawler, B. Investigating the effect of spray included angle on thermally stratified compression ignition with wet ethanol using computational fluid dynamics. *Appl. Therm. Eng.* **2020**, *170*, 114964. [CrossRef]
28. Ra, Y.; Loeper, P.; Andrie, M.; Krieger, R.; Foster, D.E.; Reitz, R.D.; Durrett, R. Gasoline DICI Engine Operation in the LTC Regime Using Triple-Pulse Injection. *SAE Int. J. Engines* **2012**, *5*, 1109–1132. [CrossRef]
29. Dempsey, A.B.; Curran, S.J.; Wagner, R.M. A perspective on the range of gasoline compression ignition combustion strategies for high engine efficiency and low NOx and soot emissions: Effects of in-cylinder fuel stratification. *Int. J. Engine Res.* **2016**, *17*, 897–917. [CrossRef]
30. Shamun, S.; Belgiorno, G.; Di Blasio, G.; Beatrice, C.; Tunér, M.; Tunestål, P. Performance and emissions of diesel-biodiesel-ethanol blends in a light duty compression ignition engine. *Appl. Therm. Eng.* **2018**, *145*, 444–452. [CrossRef]
31. Beatrice, C.; Denbratt, I.; di Blasio, G.; di Luca, G.; Ianniello, R.; Saccullo, M. Experimental assessment on exploiting low carbon ethanol fuel in a light-duty dual-fuel compression ignition engine. *Appl. Sci.* **2020**, *10*, 7182. [CrossRef]
32. Freitas, E.S.d.C.; Guarieiro, L.L.N.; da Silva, M.V.I.; Amparo, K.K.D.S.; Machado, B.A.S.; Guerreiro, E.T.d.A.; de Jesus, J.F.C.; Torres, E.A. Emission and Performance Evaluation of a Diesel Engine Using Addition of Ethanol to Diesel/Biodiesel Fuel Blend. *Energies* **2022**, *15*, 2988. [CrossRef]
33. Wallner, T. Correlation Between Speciated Hydrocarbon Emissions and Flame Ionization Detector Response for Gasoline/Alcohol Blends. *J. Eng. Gas Turbines Power* **2011**, *133*, 82801. [CrossRef]
34. Gainey, B.; Longtin, J.P.; Lawler, B. A Guide to Uncertainty Quantification for Experimental Engine Research and Heat Release Analysis. *SAE Int. J. Engines* **2019**, *12*, 509–523. [CrossRef]
35. Heywood, J.B. *Internal Combustion Engine Fundamentals*; McGraw-Hill: New York, NY, USA, 1988; ISBN 0-07-100499-8.
36. McBride, B.; Zehe, M.; Gordon, S. *NASA Glenn Coefficients for Calculating Thermodynamic Properties of Individual Species*; NASA/TP—2002-211556; NASA Glenn Research Center: Cleveland, OH, USA, 2002.
37. Dec, J.E.; Yang, Y. Boosted HCCI for High Power without Engine Knock and with Ultra-Low NOx Emissions—Using Conventional Gasoline. *SAE Int. J. Engines* **2010**, *3*, 750–767. [CrossRef]
38. Gainey, B.; Yan, Z.; Lawler, B. Autoignition characterization of methanol, ethanol, propanol, and butanol over a wide range of operating conditions in LTC/HCCI. *Fuel* **2020**, *287*, 119495. [CrossRef]
39. Dec, J.; Sjoberg, M.; Hwang, W. The Effects of EGR and its Constituents on the Autoignition of Single- and Two-Stage Fuels. In Proceedings of the 13th Diesel Engine-Efficiency and Emissions Research Conference, Detroit, MI, USA, 13–16 August 2007.
40. Dec, J.E.; Yang, Y.; Dernotte, J.; Ji, C. Effects of Gasoline Reactivity and Ethanol Content on Boosted, Premixed and Partially Stratified Low-Temperature Gasoline Combustion (LTGC). *SAE Int. J. Engines* **2015**, *8*, 935–955. [CrossRef]
41. Dempsey, A.B.; Zeman, J.; Wall, M. A System to Enable Mixing Controlled Combustion With High Octane Fuels Using a Prechamber and High-Pressure Direct Injector. *Front. Mech. Eng.* **2021**, *7*, 637665. [CrossRef]
42. Shamun, S.; Shen, M.; Johansson, B.; Tuner, M.; Pagels, J.; Gudmundsson, A.; Tunestål, P. Exhaust PM Emissions Analysis of Alcohol Fueled Heavy-Duty Engine Utilizing PPC. *SAE Int. J. Engines* **2016**, *9*, 2142–2152. [CrossRef]
43. Ithnin, A.M.; Noge, H.; Kadir, H.A.; Jazair, W. An overview of utilizing water-in-diesel emulsion fuel in diesel engine and its potential research study. *J. Energy Inst.* **2014**, *87*, 273–288. [CrossRef]
44. Yan, Z.; Gainey, B.; Gohn, J.; Hariharan, D.; Saputo, J.; Schmidt, C.; Caliari, F.; Sampath, S.; Lawler, B. A comprehensive experimental investigation of low-temperature combustion with thick thermal barrier coatings. *Energy* **2021**, *222*, 119954. [CrossRef]
45. Yan, Z.; Gainey, B.; Lawler, B. A parametric modeling study of thermal barrier coatings in low-temperature combustion engines. *Appl. Therm. Eng.* **2021**, *200*, 117687. [CrossRef]